

## Diffraction of Fast Atomic Projectiles during Grazing Scattering from a LiF(001) Surface

A. Schüller, S. Wethekam, and H. Winter\*

*Institut für Physik, Humboldt Universität zu Berlin, Brook-Taylor-Strasse 6, D-12489 Berlin-Adlershof, Germany*

(Received 27 September 2006; published 5 January 2007)

Light atoms and molecules with energies from 300 eV to 25 keV are scattered under a grazing angle of incidence from a LiF(001) surface. For impact of neutral projectiles along low index directions for strings of atoms in the surface plane we observe a defined pattern of intensity spots in the angular distribution of reflected particles which is consistently described using concepts of diffraction theory and specific features of grazing scattering of atoms from insulator surfaces. Experimental results for scattering of H, D,  $^3\text{He}$ , and  $^4\text{He}$  atoms as well as  $\text{H}_2$  and  $\text{D}_2$  molecules can be unequivocally referred to atom diffraction with de Broglie wavelengths as low as about 0.001 Å.

DOI: [10.1103/PhysRevLett.98.016103](https://doi.org/10.1103/PhysRevLett.98.016103)

PACS numbers: 68.49.Bc, 79.20.Rf, 79.60.Bm

Interference effects in the scattering of particles with finite rest mass can be understood in the framework of quantum physics only. Observation of diffraction for scattering of low energy electrons from a monocrystalline Ni surface [1] or of thermal He atoms from a LiF surface [2] were important milestones in establishing quantum mechanics. In simple terms, such diffraction effects can be envisioned by the concept of matter waves by de Broglie [3] with a wavelength for particles of mass  $M$  and velocity  $v$   $\lambda_{\text{dB}} = h/Mv$ . For electrons with energies of typically 100 eV the de Broglie wavelength is of the same order of magnitude as interatomic spacings in crystals. This makes the scattering of low energy electrons and the resulting diffraction effects (LEED) a powerful tool for studies on the structure of crystalline surfaces [4]. A similar regime is met for thermal and supersonic beams of He atoms [5] in scattering experiments from crystal targets with extreme surface sensitivity. Diffraction effects of He atoms and heavier atoms and clusters were also observed for the passage through slits of about  $\mu\text{m}$  in width in order to investigate the coherence of matter waves [6,7]. As a recent example, we mention a nozzle source with a high degree of coherence probed by slit diffraction patterns [8].

Scattering and interaction phenomena of beams of fast atoms or ions with matter are generally discussed in terms of classical mechanics. The main argument is an extremely small  $\lambda_{\text{dB}}$  compared to interatomic distances  $d$  in crystals of some Å. For example, quantum effects of  $^4\text{He}$  atoms/ions of 10 keV kinetic energy (considered as fast ion beam) can be related to  $\lambda_{\text{dB}} = 0.00143$  Å only. Then for  $\lambda_{\text{dB}}/d \approx 10^{-3}$  it is difficult to observe resulting diffraction effects, since the interaction of fast atoms/ions with matter is subject of considerable energy dissipation phenomena (electronic and nuclear stopping [9]) which would result in considerable decoherence for the impinging beams. A discussion on this topic can be found already in a paper by Bohr [10].

An interesting aspect of this problem are collisions in the channeling regime [11] where fast atoms or ions are steered by strings (“axial channeling”) or planes of lattice

atoms (“planar channeling”) in terms of small angle scattering. Under such conditions, projectile trajectories are characterized by two vastly different regimes of scattering: a “fast” one for the motion parallel to atomic strings or planes with energy  $E_{\parallel} = E_o \cos^2 \Phi_{\text{in}} \approx E_o$ , where  $E_o$  is the initial projectile energy and  $\Phi_{\text{in}}$  the glancing angle of incidence; a “slow” motion normal with respect to strings and planes with energy  $E_{\perp} = E_o \sin^2 \Phi_{\text{in}} \ll E_{\parallel}$  (for, e.g.,  $\Phi_{\text{in}} = 1$  deg holds  $E_{\perp} = 3 \times 10^{-4} E_o$ ). Since the two regimes of motion are widely decoupled it was argued that, despite high projectile energies of atomic projectiles, diffraction effects might play a role owing to the transverse motion with relatively low energy and sufficiently large de Broglie wavelengths [12].

In this Letter we discuss experiments on the grazing scattering of H and He atoms with energies up to several keV from a very clean and flat LiF(001) surface. For scattering along low indexed strings of atoms in the surface plane we observe structures in the angular distributions for scattered atoms which can be assigned to diffraction effects for fast atoms. From the analysis of diffraction patterns we deduce regimes of coherence which are closely related to the symmetry of scattering under planar as well as axial surface channeling conditions.

In our experiments we have scattered neutral He atoms (mass  $M = 3$  amu and 4 amu) as well as H atoms,  $\text{H}_2$  molecules, D atoms, and  $\text{D}_2$  molecules with energies of 300 eV to 25 keV from a clean and flat LiF(001) surface under a grazing angle of incidence of typically  $\Phi_{\text{in}} = 1$  deg. The fast neutral beams were produced via neutralization of ions in a gas cell operated with He or Kr atoms in the beam line in front of a UHV chamber (base pressure some  $10^{-11}$  mbar). The target surface was prepared by cycles of grazing sputtering with 25 keV  $\text{Ar}^+$  ions and subsequent annealing to about 350 °C. The direction of the incident beam was aligned along a  $\langle 100 \rangle$  and  $\langle 110 \rangle$  direction in the surface plane of the target, in order to achieve conditions for axial surface channeling [11,13]. Scattered projectiles are recorded at a distance of 66 cm behind the target by means of a position sensitive channel plate detector [14].

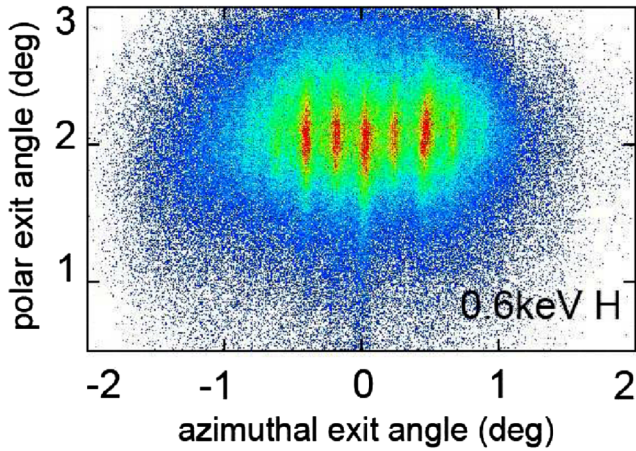


FIG. 1 (color online). Intensity distribution on position sensitive detector for scattering of 600 eV H atoms from LiF(001) along  $\langle 110 \rangle$  under  $\Phi_{in} = 2.2$  deg. Color code: red = high intensity, blue = low intensity.

In Fig. 1 we show a 2D plot of an angular distribution recorded for scattering of 0.6 keV neutral H atoms from LiF(001) under  $\Phi_{in} = 2.2$  deg. The direction of the incident beam coincides with the  $\langle 110 \rangle$  direction of the (001) plane. In the plot a number of prominent streaks can be identified. The spacings between adjacent streaks are found to be independent of  $\Phi_{in}$  at constant projectile energy  $E_o$ , but decreases with increasing  $E_o$ . The angular distribution shown in Fig. 2 for scattering of 1 keV  $^4\text{He}$  atoms under  $\Phi_{in} = 1.1$  deg reveals an even larger number of peaks.

From previous studies with metal surfaces on this topic two prominent peaks at the azimuthal rims of the angular distributions are expected [15,16]. Those peaks are interpreted in terms of “rainbow scattering” owing to the quasisinusoidal variation of the scattering potential [17]

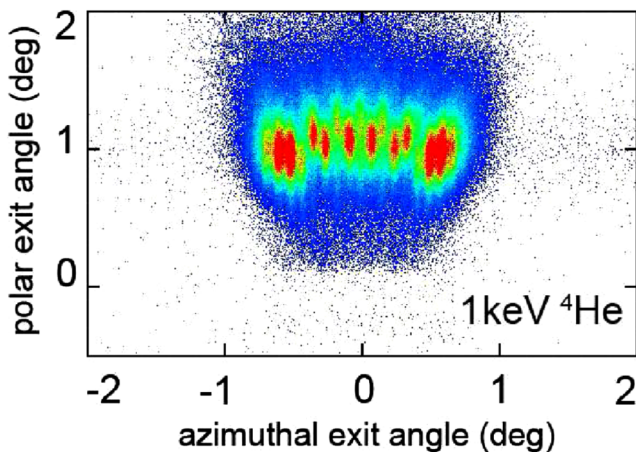


FIG. 2 (color online). Intensity distribution on position sensitive detector for scattering of 1 keV  $^4\text{He}$  atoms from LiF(001) along  $\langle 110 \rangle$  under  $\Phi_{in} = 1.1$  deg.

for axial channeling conditions. Here it is not possible to explain the observed peak structures in terms of classical scattering by corrugated potentials. In an alternative approach we analyzed our data in terms of diffraction phenomena. Such an interpretation is also motivated by the resemblance of the observed pattern with data for grazing reflection of high energy electrons (RHEED) from surfaces [18].

The general condition of constructive interference for scattering from a periodic structure in real space is that the scattering vector  $\Delta\vec{k} = \vec{k}_{out} - \vec{k}_{in}$  coincides with a reciprocal lattice vector  $\vec{g}$ . This condition can be visualized in the *Ewald construction* [4] as, e.g., applied for the analysis of diffraction spots in LEED or RHEED. In Fig. 3 we have sketched the planar reciprocal lattice (basis vectors  $\vec{g}_1$  and  $\vec{g}_2$ ) for the LiF(001) surface and the projection into this plane of the wave vector  $\vec{k}_{in}$  of the incident particle. For elastic scattering, i.e.,  $|\vec{k}_{in}| = |\vec{k}_{out}|$ , diffraction spots appear under an azimuthal angle  $\Psi$  where the tip of the outgoing wave vector  $\vec{k}_{out}$  coincides with a vector  $(\vec{g}_1, \vec{g}_2)$  of the reciprocal lattice (cf. Fig. 3).

For the data in Figs. 1 and 2 the wave vectors  $\vec{k}_{in}$  have a modulus of  $540 \text{ \AA}^{-1}$  and  $1390 \text{ \AA}^{-1}$ , respectively, which exceeds by far for LiF(001) (lattice constant  $a = 2.014 \text{ \AA}$ ) the unit for the reciprocal lattice  $g = 3.12 \text{ \AA}^{-1}$ . This is a regime comparable to RHEED and leads to similar diffraction patterns as for high energy electrons. The azimuthal angle between the (00) and a (11) spot derived for 600 eV H atoms from the construction sketched in Fig. 3 is  $\Psi \approx \sqrt{2}g/k_{in} = 0.46$  deg which is consistent with twice the

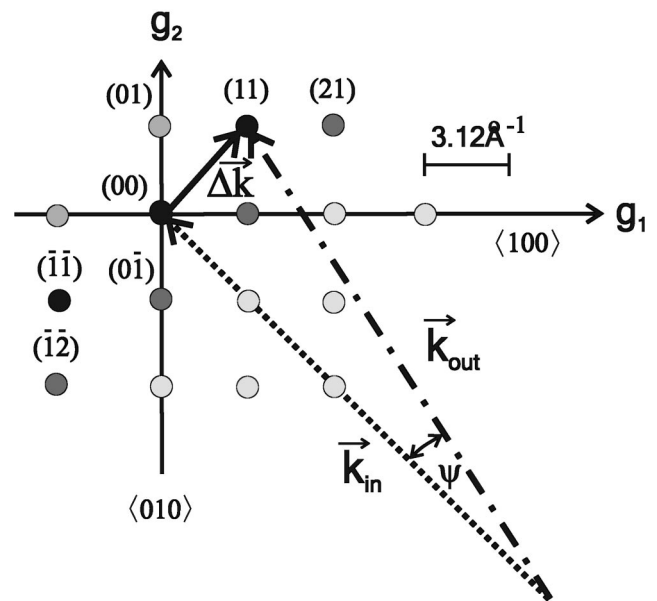


FIG. 3. Ewald construction for the reciprocal lattice of the surface plane of LiF(001). Note that lengths of vectors  $k_{in}$ ,  $k_{out}$  do not scale. For details, see text.

angular splitting between adjacent peaks  $\Delta\Psi = (0.22 \pm 0.02)$  deg in Fig. 1. We therefore interpret the data displayed in Fig. 1 as  $(\bar{1}\bar{1})$ ,  $(00)$ ,  $(11)$  reflexes. The  $(0\bar{1})$ ,  $(10)$  reflexes in Fig. 1 appear at slightly larger exit angles in between. This feature is more pronounced in the data for 1 keV  $^4\text{He}$  (cf. Fig. 2) where the smaller de Broglie wavelength of  $4.5 \cdot 10^{-3}$  Å results in smaller angular spacings between streaks which are in quantitative accord with the calculations. For the higher energy we reveal an azimuthal intensity modulation for the streak pattern (cf. Fig. 2).

For a more detailed investigation we scattered H, D,  $^3\text{He}$ , and  $^4\text{He}$  atoms as well as  $\text{H}_2$  and  $\text{D}_2$  molecules from LiF(001) along the  $\langle 100 \rangle$  and  $\langle 110 \rangle$  directions. In Fig. 4 we have plotted the azimuthal angular shift between adjacent diffraction streaks as function of  $\lambda_{\text{dB}}$  for the different projectiles. We find for both azimuthal directions the expected linear behavior. A best fit to the two data sets by a linear dependence yields slopes of  $(28.7 \pm 0.9)$  deg/Å ( $\langle 100 \rangle$ ) and  $(20.1 \pm 0.7)$  deg/Å ( $\langle 110 \rangle$ ). This agrees well with the values of  $28.5$  deg/Å and  $20.1$  deg/Å, calculated from  $\Psi = g/2\pi \cdot \lambda_{\text{dB}}$  and  $\Psi = g/\sqrt{22}\pi \cdot \lambda_{\text{dB}}$ , respectively. We conclude that the observed diffraction patterns result from the coherence of the atomic beam during scattering from the planar arrangement of lattice atoms of the crystal surface. This compares to the conditions for RHEED.

A closer inspection of Fig. 2 reveals that the diffraction pattern is located on a circle of radius  $\Phi_{\text{in}}$  and shows high intensities for the two outermost peaks. Both features are attributed to the symmetry for scattering under axial surface channeling, where projectile trajectories are steered along strings of surface atoms by a scattering potential of axial symmetry. This results in an intensity distribution of circular shape with an extremum in deflection angle, the

so-called *rainbow angle*. For this angle the differential cross section and the intensity of scattered projectiles is enhanced (cf. pronounced outermost peaks in Figs. 2 and 5). In passing we note that this type of scattering provides a sensitive tool for studies on atomic interaction potentials at surfaces [15,16,19]. This regime of scattering plays an important role for the observation of diffraction effects for fast atoms, since scattering of projectiles out of the collision plane leads to an intensity enhancement for scattering into angles of higher diffraction orders than zero, similar to the role of blazing for the grating of an optical spectrometer or the diffraction of thermal He atoms from a vicinal Pt(997) surface [20].

The second important aspect is the separation of the motion of projectiles parallel and normal to atomic strings for axial surface channeling. Then for grazing angles with respect to a string the normal motion proceeds with velocity  $v_{\perp} = v_o \sin\Phi_{\text{in}}$  and a correspondingly reduced de Broglie wavelength by a factor  $\sin\Phi_{\text{in}}$ , typically 2 orders of magnitude smaller than  $\lambda_{\text{dB}}$  for  $v_o$  of the incident atom. The condition for constructive interference in a plane normal to atomic strings is  $n\lambda_{\text{dB}}/\sin\Phi_{\text{in}} = d \sin\Theta$  with  $d$  being the distance between adjacent atomic strings and  $n$  the diffraction order.  $\Theta$  denotes the scattering angle in the plane normal to strings, and diffraction spots appear for  $\sin\Theta = n(\lambda_{\text{dB}}/d)/\sin\Phi_{\text{in}}$ . As a consequence, the diffraction angle for a given ratio  $\lambda_{\text{dB}}/d$  is enhanced by a factor  $1/\sin\Phi_{\text{in}}$ . In Fig. 5 we show the angular distribution for 3 keV  $^3\text{He}$  atoms scattered under  $\Phi_{\text{in}} = 1.1$  deg ( $E_{\perp} = 1.1$  eV) along  $\langle 110 \rangle$  where a fair number of diffraction spots can be identified. The high intensity for the outermost peaks is due to rainbow scattering. Compared to the diffraction patterns at lower projectile energies (larger  $\lambda_{\text{dB}}$ ) in Figs. 1 and 2, the pattern shows axial symmetry with respect to  $\langle 110 \rangle$  strings, and streaks owing to the planar lattice are no longer resolved. The angular positions of

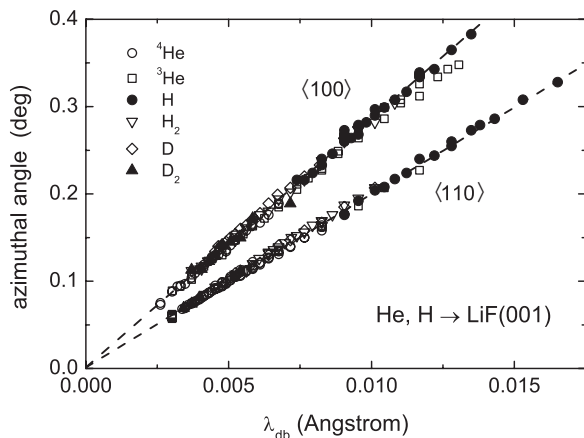


FIG. 4. Azimuthal angular splitting  $\Delta\Psi$  as function of de Broglie wavelength for scattering of H (●), D (◇),  $^3\text{He}$  (□),  $^4\text{He}$  (○),  $\text{H}_2$  (△),  $\text{D}_2$  (▲) from LiF(001) along  $\langle 100 \rangle$  (upper curve) and  $\langle 110 \rangle$  (lower curve). Dashed lines: best fit to linear dependence  $\Psi$  vs  $\lambda_{\text{dB}}$ .

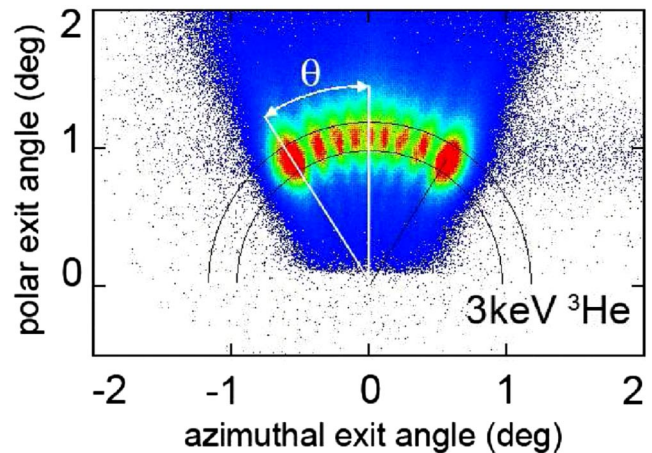


FIG. 5 (color online). Intensity distribution on position sensitive detector for scattering of 3 keV  $^3\text{He}$  atoms from LiF(001) along  $\langle 110 \rangle$  under  $\Phi_{\text{in}} = 1.1$  deg. Circles with origin at direction of atomic surface strings mark interval of angles around  $\Phi_{\text{in}}$ .

peaks are observed to be independent of  $E_o$  for constant  $E_{\perp}$  up to projectile energies of about 20 keV. For a detailed analysis of diffraction pattern as shown in Fig. 5 the corrugation of the scattering potential at the surface has to be taken into account which leads to a modulation of intensities of diffraction spots.

In contrast to our studies with fast neutral atoms we did not observe diffraction effects with incident ions. This result is closely related to specific features concerning the dissipation of projectile energy during grazing scattering from insulator surfaces. Since for neutral atoms with keV energies electronic excitations are negligible, the energy loss for light atoms owing to binary collisions with surface atoms under large impact parameters amounts to less than 1 eV [21]. As a consequence, the energy (velocity) of the incident atoms is almost unchanged and well defined during and after scattering. For scattering of ions, however, Coulomb excitations of optical phonons play an important role resulting in energy loss and straggling of some 10 eV [22]. In simple terms, this latter process leads to a smearing out of the wave vectors for the scattered particles so that the substantial decoherence does no longer allow one to detect diffraction effects. In this respect one might detect diffraction of fast atoms also for scattering from semiconductors, but we do not expect such effect for scattering from metal surfaces, where electronic excitations are already substantial for grazing scattering in the keV domain.

In conclusion, we have observed atom diffraction for the scattering of fast light neutral atoms and molecules from a LiF(001) surface. In a regime of atomic collisions where so far trajectories of scattered projectiles have been described by classical concepts, we find signatures which can be unequivocally attributed to quantum mechanical effects. We observe two kinds of diffraction effects which are closely related to specific features of axial surface channeling. For kinetic energies of typically some 100 eV the coherence results in diffraction from the planar surface lattice comparable to, e.g., RHEED, whereas for projectile energies in the keV domain the slow transverse motion (transverse coherence) with respect to atomic strings might lead to the observation of diffraction patterns for  $\lambda_{dB}$  as low as  $10^{-4}$  Å and possibly lower. A particular potential of our work are studies on decoherence phenomena relevant for the transition from quantum to classical scattering. Such phenomena could be studied under our conditions of scattering in detail. In this respect a more refined analysis of the diffraction pattern provides valuable information on the scattering process.

We thank the DFG (Project No. Wi 1336) for financial support, and K. Maass and J. Sölle for their assistance in the preparation of the experiments.

*Note added in proof.*—During completion of our studies we learned of similar work performed by Roncin *et al.* [23].

---

\*Author to whom correspondence should be addressed.

Email address: winter@physik.hu-berlin.de

- [1] C. Davisson and L. H. Germer, *Phys. Rev.* **30**, 705 (1927).
- [2] I. Estermann and A. Stern, *Z. Phys.* **61**, 95 (1930).
- [3] L. V. de Broglie, *Comptes rendus de l'Academie bulgare des sciences : sciences mathematiques et naturelles* **177**, 507 (1923).
- [4] A. van Hove, W.H. Weinberg, and C.M. Chan, *Low Energy Electron Diffraction* (Springer, New York, 1986).
- [5] B. Poelsema and G. Comsa, *Springer Tracts in Modern Physics* (Springer, New York, 1989), Vol. 115.
- [6] O. Carnal and J. Mlynek, *Phys. Rev. Lett.* **66**, 2689 (1991).
- [7] M. Arndt, O. Nairz, J. Vos-Andreae, C. Keller, G. van der Zouw, and A. Zeilinger, *Nature (London)* **401**, 680 (1999).
- [8] F. S. Patton, D. P. Deponte, G. S. Elliott, and S. D. Kevan, *Phys. Rev. Lett.* **97**, 013202 (2006).
- [9] J. F. Ziegler, J. P. Biersack, and U. Littmark, *The Stopping and Range of Ions in Solids* (Pergamon, New York, 1990).
- [10] N. Bohr, *Dan. Vidensk. Selsk. Mat. Fys. Medd.* **18**, 8 (1948).
- [11] D. Gemmell, *Rev. Mod. Phys.* **46**, 129 (1974).
- [12] M. W. Thompson, in *Channeling*, edited by D. V. Morgan (Wiley, New York, 1973), p. 1.
- [13] H. Winter, *Phys. Rep.* **367**, 387 (2002).
- [14] Roentdek GmbH, Kelkheim-Ruppertsheim, Germany.
- [15] A. Schüller, G. Adamov, S. Wethekam, K. Maass, A. Mertens, and H. Winter, *Phys. Rev. A* **69**, 050901(R) (2004).
- [16] A. Schüller, S. Wethekam, A. Mertens, K. Maass, H. Winter, and K. Gärtner, *Nucl. Instrum. Methods Phys. Res., Sect. B* **230**, 172 (2005).
- [17] A. W. Kleyn and T. C. M. Horn, *Phys. Rep.* **199**, 191 (1991).
- [18] J. E. Mahan, K. M. Geib, G. Y. Robinson, and R. G. Long, *J. Vac. Sci. Technol. A* **8**, 3692 (1990).
- [19] D. Danailov, K. Gärtner, and A. Caro, *Nucl. Instrum. Methods Phys. Res., Sect. B* **153**, 191 (1999).
- [20] G. Comsa, G. Mechtersheimer, and B. Poelsema, *Surf. Sci.* **97**, L297 (1980).
- [21] A. Mertens and H. Winter, *Phys. Rev. Lett.* **85**, 2825 (2000).
- [22] A. G. Borisov, A. Mertens, H. Winter, and A. K. Kazansky, *Phys. Rev. Lett.* **83**, 5378 (1999).
- [23] P. Roncin *et al.*, this issue, *Phys. Rev. Lett.* **98**, 016104 (2007).